Article

An essential role for the latero-medial secondary visual cortex in the acquisition and retention of visual perceptual learning in mice

Alan Consorti [1,2,3], Gabriele Sansevero [1,3], Irene Di Marco[1,2], Silvia Floridia [1], Elena Novelli[1], Nicoletta Berardi[1,2] & Alessandro Sale [1]✉

Perceptual learning refers to any change in discrimination abilities as a result of practice, a fundamental process that improves the organism's response to the external environment. Visual perceptual learning (vPL) is supposed to rely on functional rearrangements in brain circuity occurring at early stages of sensory processing, with a pivotal role for the primary visual cortex (V1). However, top-down inputs from higher-order visual areas (HVAs) have been suggested to play a key part in vPL, conveying information on attention, expectation and the precise nature of the perceptual task. A direct assessment of the possibility to modulate vPL by manipulating top-down activity in awake subjects is still missing. Here, we used a combination of chemogenetics, behavioral analysis and multichannel electrophysiological assessments to show a critical role in vPL acquisition and retention for neuronal activity in the latero-medial secondary visual cortex (LM), the prime source for top-down feedback projections reentering V1.

The functional properties of visual cortical neurons are not fixed but are continuously modulated by top-down information relative to the behavioral context. Such influences convey higher-order signals that add to the bottom-up input of feedforward connections carrying information on basic sensory aspects of the external world[1,2]. This top-down signal is considered to take part in allowing a stable representation of the sensory environment, despite the continuous subject movements[3,4], and to have a major role in the encoding and recall of learned information[5,6].

A paradigmatic case is that of visual perceptual learning (vPL), i.e. an increase in visual perceptual abilities as a result of experience and practice[7–9]. vPL can occur in response to a wide range of visual tasks, including discrimination of orientation[10,11], texture[12], visual gratings[13–16], changes in spatial frequency[17], small depth differences between two targets[18], and even face recognition[19]. Classical electrophysiological, neuroimaging and psychophysical observations have led to the assumption that the primary visual cortex (V1) has a dominant role in vPL. Accordingly, vPL is highly specific for the trained location[10,12,15,20,21] and stimulus orientation[10,12,15,22–25], a characteristic typical of V1 neurons[26,27]. In agreement with this view, several electrophysiological and functional imaging studies reported that visual perceptual improvements correlate with changes in the visual representation of V1, both in humans[28–31] and animal models[32–35].

Despite the pivotal role of V1, top-down inputs from higher-order visual areas (HVAs) are also thought to play a key part in vPL[36]. Indeed, during vPL, visual cortical neurons are subjected to top-down influences conveying information of attention, expectation and the precise nature of the visual task. In a series of seminal studies, the group of Gilbert and colleagues investigated top-down processing in vPL by means of bisection tasks. These tasks involve the localization of short line segments and examine the specificity of the learning for the visual location, orientation, and geometric arrangement of the trained

[1]Neuroscience Institute, National Research Council (CNR), Pisa, Italy. [2]NEUROFARBA, University of Florence, 50139 Florence, Italy. [3]These authors contributed equally: Alan Consorti, Gabriele Sansevero. ✉e-mail: sale@in.cnr.it

stimulus[32,33,37,38]. To specifically dissect the role of top-down processing, these authors recorded the electrical activity of V1 neurons in a group of anesthetized monkeys after vPL practice[33]. Inhalation of anesthetics, a process that preferentially reduces the activity of top-down connections[39–42], completely abolished V1 changes induced by vPL[33]. Similarly, transient chemical inhibition of the monkey middle temporal area impaired perceptual performance on a coarse-depth discrimination task[43]. In humans, a transient interference with the middle temporal area or the posterior parietal cortex activity was also reported to affect the performance in different discrimination tasks[44,45].

Despite the evidence coming from primate studies and pointing toward a crucial involvement of top-down integration in vPL, a direct assessment of the possibility to modulate vPL by manipulating top-down activity in awake subjects and with a direct control of neuronal activity during the learning trials is still missing. To fill this gap, here we employed a mouse model of vPL recently developed in our laboratory, in which mice were trained in a forced-choice visual task consisting in the discrimination of two vertical gratings, differing only for their spatial frequency. This task, inspired by the classical work by Fiorentini and Berardi (1980)[22], was adapted by Sale et al.[46] for application to rodents. Using this task, we have previously shown that vPL correlates with specific plastic changes in V1 activity. To investigate the possible involvement of higher order visual areas, we focused our attention on the latero-medial secondary visual cortex (LM), the homologous of the primate secondary visual cortex (V2)[47–49], considered the prime source for top-down feedback projections reentering V1[36,50], and the gateway of the ventral visual stream[51]. Alterations in the activity of areas belonging to this pathway have been previously associated with learning and perceptual deficits[52–55]. Nevertheless, the involvement of the ventral visual stream in vPL remained to be addressed. Using a combined approach based on chemogenetics, behavioral analysis and multichannel electrophysiological recordings, we provide strong evidence for an essential role of LM not only in vPL acquisition but also in its retention.

Results
Visual perceptual learning in mice
A group of mice ($n = 14$) was subjected to a vPL protocol in which they were asked to discriminate two vertical gratings with equal contrast, but different spatial frequency (SF), made progressively more similar by making their SF closer to each other. Initially, the test grating had a SF of 0.522 c/deg, while the reference grating had a SF of 0.116 c/deg. All mice easily learned this discrimination task, with the percentage of correct choices increasing over the course of the training sessions (One-way RM ANOVA, Holm-Sidak method, $F = 24.276$, DF = 1, $p < 0.001$) and finally achieving a performance level of at least 80% of accuracy in at least three subsequent sessions (Fig. 1a). At this point, mice were divided in two groups: vPL mice ($n = 7$) underwent a perceptual learning task, practicing with a progressively more difficult discrimination as the SF of the test grating was made increasingly more similar to that of the reference grating; the other group, First-Step (FS) mice, ($n = 7$) continued to practice with the test grating maintained at the starting value of 0.522 c/deg. Notably, no differences were found in visual discrimination abilities between prospective FS and vPL mice during the initial phase (Two-way RM ANOVA, Holm–Sidak method, $F = 1.334$, DF = 1, $p = 0.346$, Fig. 1b).

In vPL mice, we observed a robust improvement in visual discrimination abilities with practice, as shown by the progressive reduction in the minimum spatial frequency discrimination threshold (MDT) across sessions. In the first session, mean MDT was 0.282 ± 0.016 c/deg, while this value reached 0.043 ± 0.004 c/deg at the end of the vPL training procedure (One-way RM ANOVA on ranks, $p < 0.001$, Fig. 1c). A clear vPL was also revealed by the increase in the percentage of correct choices for a given SF of the test grating (for example: reference grating of 0.116 c/deg vs test grating of 0.160

c/deg, $n = 7$, One-way RM ANOVA, Holm–Sidak method, $F = 14.691$, DF = 2, $p < 0.001$). In FS mice, the performance remained stable (Fig. 1d).

A separate group of animals was used to probe the difference in the vPL task between male and female mice ($n = 16$, 8 males and 8 females). No difference could be found either in the achieved MDT (males: 0.044 ± 0.003 c/deg, females: 0.039 ± 0.004; t test, $t = 0.794$, DF = 14, $p = 0.441$, Supplementary Fig. 1a) and the acquisition rate of the vPL (Two-way RM ANOVA, Holm–Sidak method, $F = 0.521$, DF = 1, $p = 0.428$, Supplementary Fig. 1b)

To test the specificity of vPL for the stimulus orientation, we performed, in the same vPL mice previously trained with vertical stimuli ($n = 7$), an experiment of orientation shift in which the two vertical gratings were rotated by 90°; afterwards, new trials were applied to assess the new MDT. We found that the visual grating discrimination abilities achieved by vPL mice were highly selective for the orientation of the stimulus; indeed, we found a marked impairment in their discrimination abilities occurring immediately after the rotation of the stimuli ($n = 7$, MDT before shift: 0.040 ± 0.004 c/deg, DT after shift: 0.327 ± 0.021 c/deg; paired t test, $t = -13.084$, DF = 6, $p < 0.001$, Fig. 2a, b). The animals appeared unable to discriminate the newly oriented stimuli when the test grating was maintained at the same SF reached before the orientation shift, and the percentage of correct choices fell below the 70% criterion for two consecutive vPL sessions (gray bars, Fig. 2a), until a higher SF difference between the two stimuli was achieved. With additional training, the animal performance reached a new perceptual plateau, and the MDT for horizontal grating was not significantly different from that achieved before the stimulus orientation change ($n = 7$, MDT before shift: 0.040 ± 0.004 c/deg, MDT after shift and vPL training: 0.040 ± 0.004 c/deg; paired t test on ranks, $p = 1.000$; Fig. 2a, c). In contrast, FS mice were still able to perform the task when the two vertical gratings were rotated by 90° (MDT before shift: $100\% \pm 0.0\%$; MDT after shift: $91\% \pm 0.035\%$; paired t test on ranks, $p = 0.125$; see Supplementary Fig. 2).

Electrophysiological characterization of LM activity
To provide a general characterization of basic LM neuronal activity features, visual evoked potentials (VEPs) and single-units were recorded in a group of anesthetized naïve mice ($n = 7$), by means of multichannel electrophysiological recordings. VEP recordings represent the elective method to study the function of visual areas and they have been extensively employed to assess visual capabilities, local cortical processing and the state of maturation of visual pathways[56–59]. Single-unit recordings were instead employed to locally characterize electrical responses of LM neurons.

To assess visual acuity, VEP responses were recorded from a silicon electrode inserted 3.6 mm lateral to lambda and advanced 200 μm within the cortex, in response to horizontal gratings of different SFs and maintained at 90% contrast. VEP acuity was obtained extrapolating VEP amplitude to 0 V. The average acuity was 0.408 ± 0.039 c/deg (Supplementary Fig. 3a). LM VEP acuity is just a measure of spatial resolution in LM visual neurons, but it does not necessarily reflect visual acuity in mice, as this requires recordings to be performed from V1. To measure contrast sensitivity, VEPs were recorded in response to gratings of a spatial frequency of 0.06 c/deg, at different contrasts. Contrast sensitivity was obtained extrapolating to 0 V the recorded VEP amplitudes. The average contrast threshold was $9.46\% \pm 2.051\%$ (Supplementary Fig. 3b).

To further characterize the electrical activity of LM neurons, single units in response to drifting sinusoidal gratings were recorded at multiple depths, spanning all cortical layers. Single units were clustered in seven ocular dominance (OD) classes on the basis of the ratio of contralateral to ipsilateral peak responses, according to the Hubel & Wiesel's classification[60]. The great majority of all recorded cells ($n = 145$) fell into the intermediate OD classes, without a prevalence of
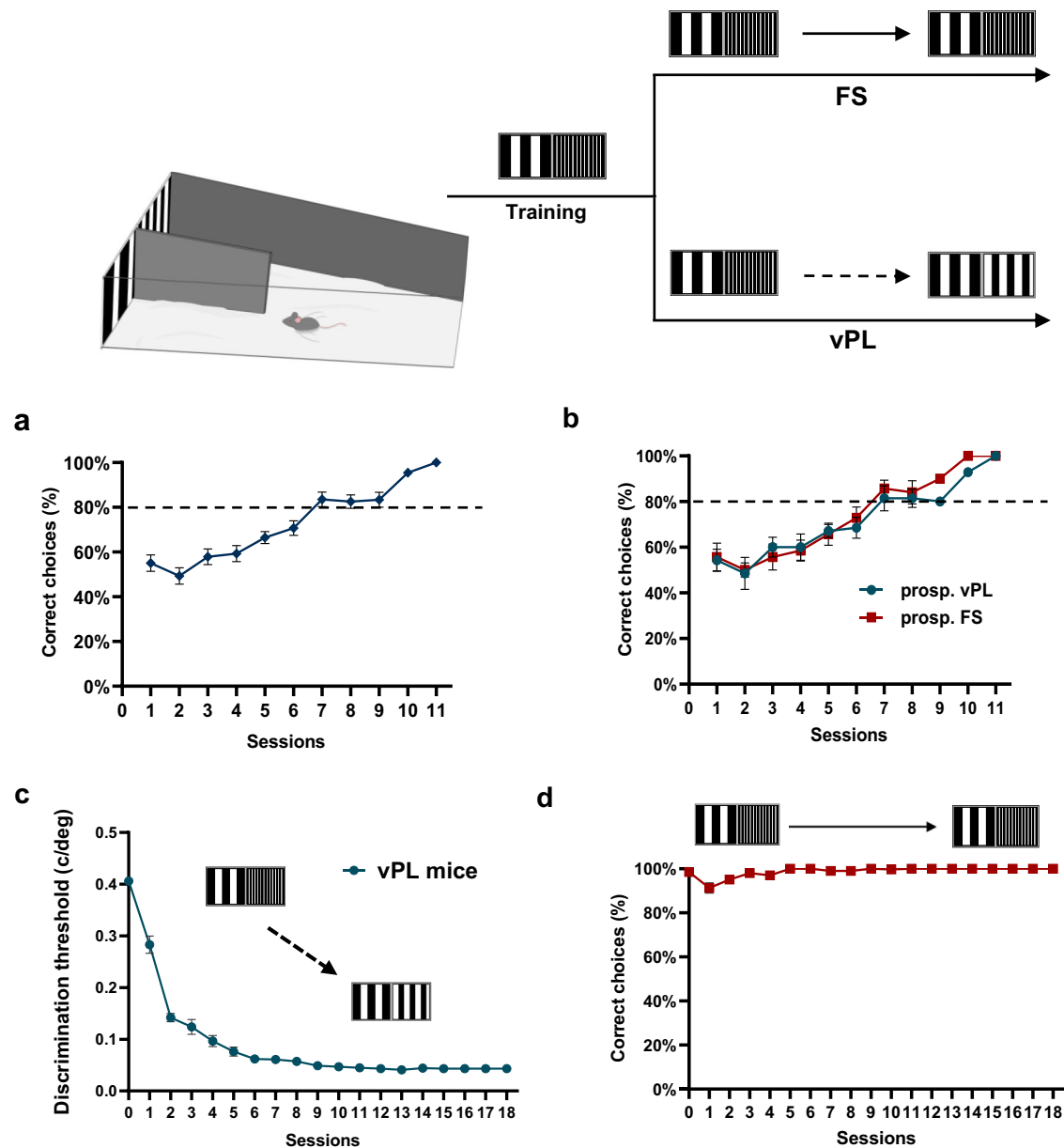
Fig. 1 | A mouse model of vPL. A modified version of the visual water box task was used to perform vPL. **a** Mean performance in distinguishing a test grating of 0.522 c/deg from the reference grating of 0.116 c/deg across the training sessions. All animals ($n = 14$, vPL and FS mice) have been pooled together. The increase in the percentage of correct choices with sessions was significant (One-way RM ANOVA, Holm−Sidak method, $p < 0.001$). **b** During training, the percentage performance of prospective (prosp.) FS mice ($n = 7$) was not different compared to the training performance of prosp. vPL mice ($n = 7$, Two-way RM ANOVA, Holm−Sidak method, $p = 0.346$). **c** Improvement of discrimination threshold in vPL mice engaged in the vPL task. The threshold, calculated as the minimum spatial frequency difference between the reference and the test gratings, decreased significantly across training days ($n = 7$, One-way RM ANOVA on ranks $p < 0.001$). **d** After few sessions, the performance of FS mice ($n = 7$) engaged in a simple discrimination task remained stable across the training days. *Statistical significance. Error bars, s.e.m. Source data are provided as a Source Data file.

either the contralateral (class 1) or the ipsilateral (class 7) eye (Fig. 3a). LM electrical activity was evaluated measuring spontaneous (contra = 0.220 Hz, ipsi = 0.274 Hz, Fig. 3b) and evoked discharge (contra = 3.008 Hz, ipsi = 2.502 Hz, Fig. 3c), while orientation and direction selectivity were assessed calculating the orientation selectivity index (OSI, contra = 0.465, ipsi = 0.565, Fig. 3d) and direction selectivity index (DSI, contra = 0.225, ipsi = 0.210, Fig. 3e). No difference was found in the electrical activity recorded from the contralateral and ipsilateral eye in the spontaneous discharge or DSI ($n = 6$, paired t test, DF = 5, $t = -1.242$ $p = 0.269$; $t = -0.0298$ $p = 0.977$, respectively) nor in the evoked discharge and OSI ($n = 7$, paired t test, DF = 6, $t = 2.212$ $p = 0.069$; $t = -1.800$ $p = 0.122$, respectively).

Chemogenetic inhibition of LM activity
In order to silence global LM neuronal activity, a constitutive viral vector was injected into the LM of naïve mice, to induce the expression of hM4D(Gi)-mCherry, an inhibitory DREADD (designer receptors activated exclusively by designer drugs). Histological evaluations showed that the expression of hM4D(Gi)-mCherry was confined into LM, without entering the dorsal visual stream (Fig. 4).

Two weeks after the injection of the viral vector, single units were recorded from LM in a group of mice ($n = 9$), to probe the effective chemogenetic inhibition of LM activity. In a group of mice ($n = 5$), electrical signals in response to alternate monocular stimulation of the two eyes were recorded before and 15 min after an intraperitoneal (i.p.)
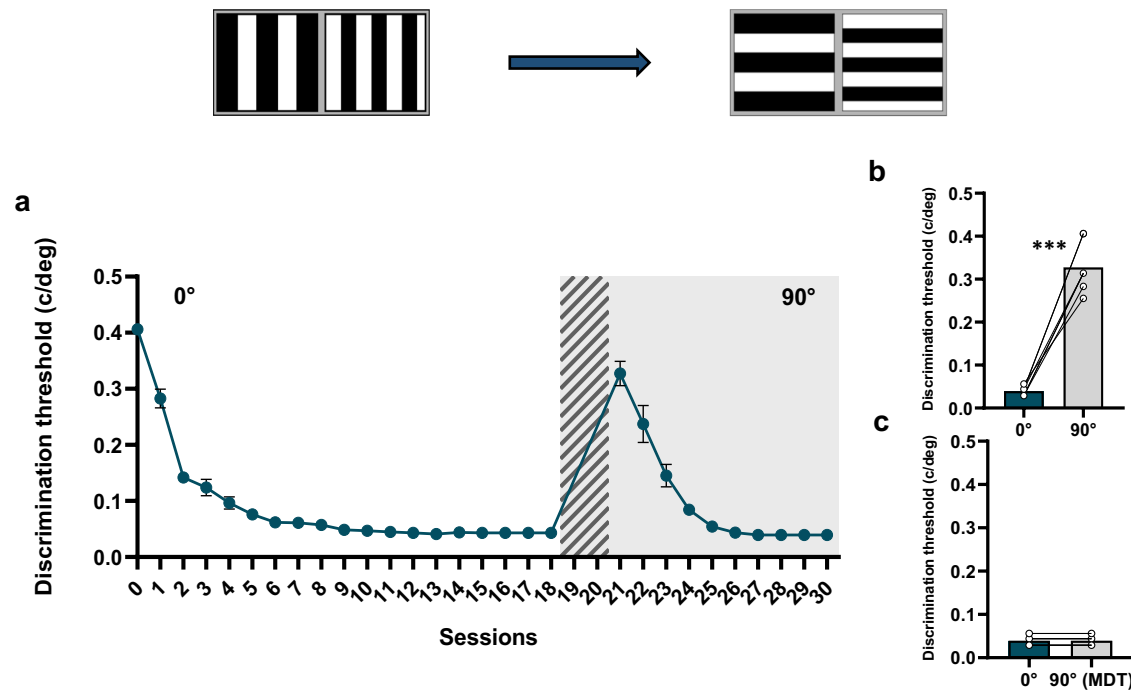
Fig. 2 | Orientation shift in vPL mice. When vPL mice achieved their minimum spatial frequency discrimination threshold (MDT), the reference and test gratings were rotated by 90° keeping fixed their spatial frequency difference. **a** vPL mice ($n = 7$) were subjected to a simple incremental discrimination task until the MDT was achieved. The stimuli were then rotated by 90°. vPL mice were totally unable to discriminate the newly oriented stimuli for two consecutive sessions (performance drop below the criterion of at least 70% correct choices, gray bars). However, when additional vPL training was applied, vPL mice reached the same perceptual plateau achieved before the orientation shift. **b** vPL mice were totally unable to discriminate the newly oriented stimuli ($n = 7$, MDT before shift: 0.040 ± 0.004 c/deg, DT after shift: 0.327 ± 0.021 c/deg; two-tailed paired t test, $p < 0.001$). **c** Starting from this point, additional vPL training was applied. The new performance plateau was not significantly different from that achieved before the stimulus orientational shift ($n = 7$, MDT before shift: 0.040 ± 0.004 c/deg, MDT after shift and vPL training: 0.040 ± 0.004 c/deg; two-tailed paired t test, $p = 1.000$). *Statistical significance. Error bars, s.e.m. Source data are provided as a Source Data file.

administration of Clozapine N-oxide (CNO), a DREADD ligand. We found that CNO administration resulted in a marked suppression of the evoked activity in response to both the contralateral (pre-CNO = 2.473 ± 0.690 Hz, post-CNO = 0.789 ± 0.112 Hz; paired t test, $t = 3.039$, DF = 4, $p = 0.038$, Fig. 5a) and ipsilateral (pre-CNO = 2.559 ± 0.597 Hz, post-CNO = 0.415 ± 0.188 Hz; paired t test, $t = 4.180$, DF = 4, $p = 0.014$, Fig. 5a) eye stimulation. In contrast, no reduction in LM evoked activity was found in control mice ($n = 4$) recorded before (pre-SAL; contra = 1.708 ± 0.325 Hz, ipsi = 1.681 ± 0.294 Hz) and 15 min after an i.p. administration of saline (post-SAL; contra = 1.87 ± 0.358 Hz, ipsi = 1.274 ± 0.288 Hz) (paired t test, contra: on ranks, $p = 0.375$ and ipsi: $t = 0.734$, $p = 0.516$, Fig. 5b). Notably, LM activity recorded from CNO and SAL mice was statistically different after the i.p. administration (post CNO vs post-SAL, t test, DF = 7, contra: $t = -3.242$, $p = 0,014$ and ipsi: $t = -2.733$, $p = 0.029$). In contrast, no difference could be found between the two groups of mice before the i.p. administration of CNO or saline, respectively (pre CNO vs pre SAL, t test, DF = 7, contra: $t = 1.020$, $p = 0.342$ and ipsi: $t = 1.342$, $p = 0.221$).

To evaluate the global impact of the hM4D injection, single-unit activity recorded from CNO and SAL mice was compared to that sampled from naïve animals ($n = 6$). Only the evoked responses recorded from the contralateral and ipsilateral eyes of the animals treated with CNO (post-CNO) were significantly different compared to the responses recorded from naïve mice (Naïve, contra = 2.659 ± 0.354 Hz ipsi = 2.421 ± 0.603 Hz) (One-way ANOVA vs control, Holm−Sidak method, DF = 4, contra: $F = 3.791$, $p = 0.02$ and ipsi: $F = 3.919$, $p = 0.031$, Fig. 5c).

LM activity is required for vPL acquisition

Then, we used the same chemogenetic approach to test whether suppression of LM activity was able to significantly affect vPL. A group

of mice ($n = 16$) was required to learn the vPL task two weeks after the hM4D injection. Once the 80% criterion was achieved, a subgroup of animals was subjected to the incremental phase of vPL with administration of CNO ($n = 8$, CNO mice), while a second subgroup of animals were tested on the same task with administration of saline ($n = 8$, SAL mice). Injections of either CNO or saline were performed 30 min before each vPL session. The performance plateau reached by CNO mice (0.180 ± 0.029 c/deg) was significantly different from that achieved by SAL mice (0.042 ± 0.004 c/deg), with the former group of animals displaying a robust learning impairment both in the slope of the vPL curve and in the achieved perceptual plateau (Two-way RM ANOVA on ranks, Holm−Sidak method, $p < 0.001$, Fig. 6a).

The perceptual learning performance of CNO mice, but not that of SAL mice, was consistently different from the performance displayed by naïve animals subjected to the same vPL task (Two-way RM ANOVA on ranks, Holm-Sidak method, vPL mice vs CNO mice: $p < 0.001$; vPL mice vs SAL mice $p = 0.513$; SAL mice vs CNO mice: $p < 0.001$; Fig. 6a), with CNO mice reaching a significantly higher MDT compared to both SAL and vPL mice (One way ANOVA on ranks, Dunn's method, $p < 0.001$). Notably, no differences could be found between mice that were administered with CNO (prospective CNO) or with saline (prospective SAL) during the learning phase of the discrimination task (Two-way RM ANOVA, Holm−Sidak method, $F = 0.0980$, DF = 1, $p = 0.757$, Fig. 6b). Moreover, the learning capabilities of the entire group of injected mice ($n = 16$) were not different from those of naïve mice ($n = 14$, vPL and FS mice pooled together), ruling out the possibility that the observed impairment in vPL animals could be dependent to learning deficits due to the surgical procedures per se (Two-way RM ANOVA, Holm−Sidak method, $F = 1.694$, DF = 1, $p = 0.200$, Fig. 6c).

To rule out the possibility that the deficits observed in CNO mice might be due to a visual impairment caused by the manipulation of LM
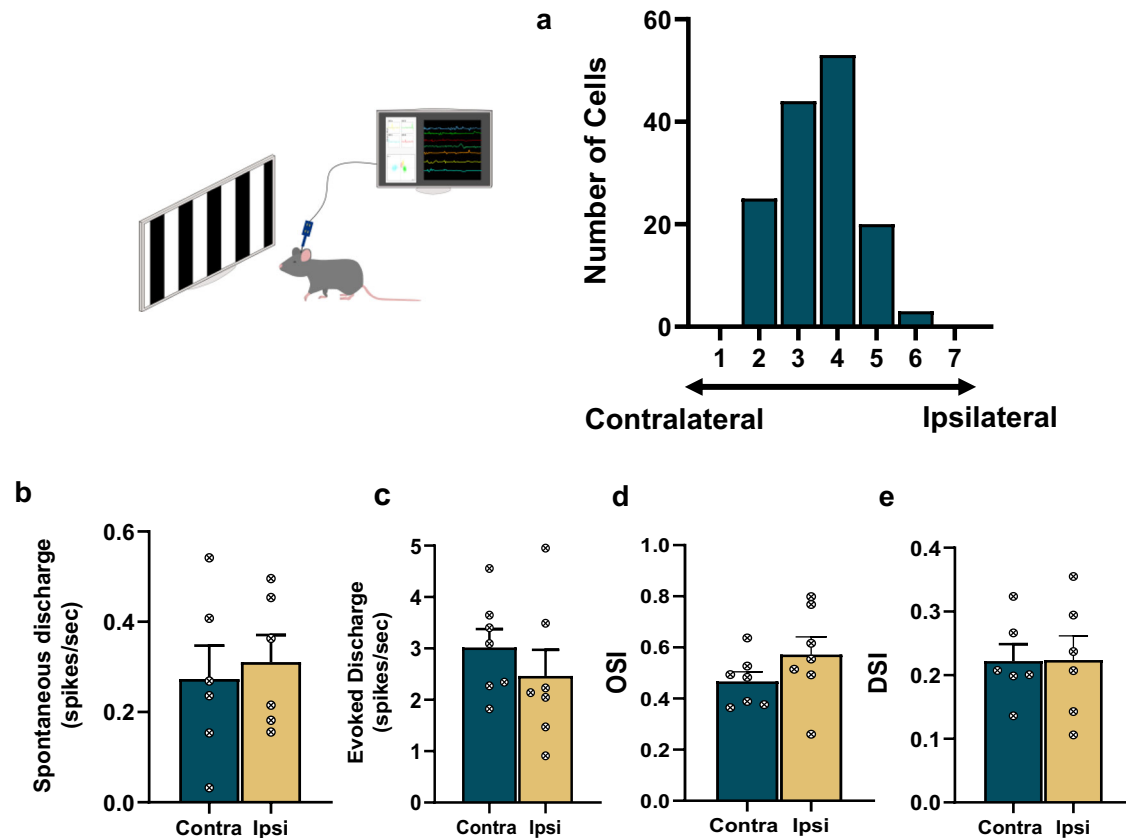
Fig. 3 | Single unit recordings from the LM. Single units were recorded in a group of naïve animals sampling at different cortical depths. **a** In order to assess LM binocularity, sorted cells were clustered in 7 ocular dominance classes according to the contralateral/ipsilateral response. Then, to characterize LM activity, the spontaneous and evoked activities (**b** and **c**, respectively), the orientation selectivity and the direction selectivity indices (**d** and **e**, respectively) were measured in all sorted units. For all the recorder parameters, no difference was found in the electrical activity measured in response to the contralateral or ipsilateral eye stimulation ($n = 7$, paired t test: $p = 0.269$, $p = 0.069$, $p = 0.122$, $p = 0.122$, respectively). Single dots were obtained averaging all the single units recorded in each animal. *Statistical significance. Error bars, s.e.m. Source data are provided as a Source Data file.
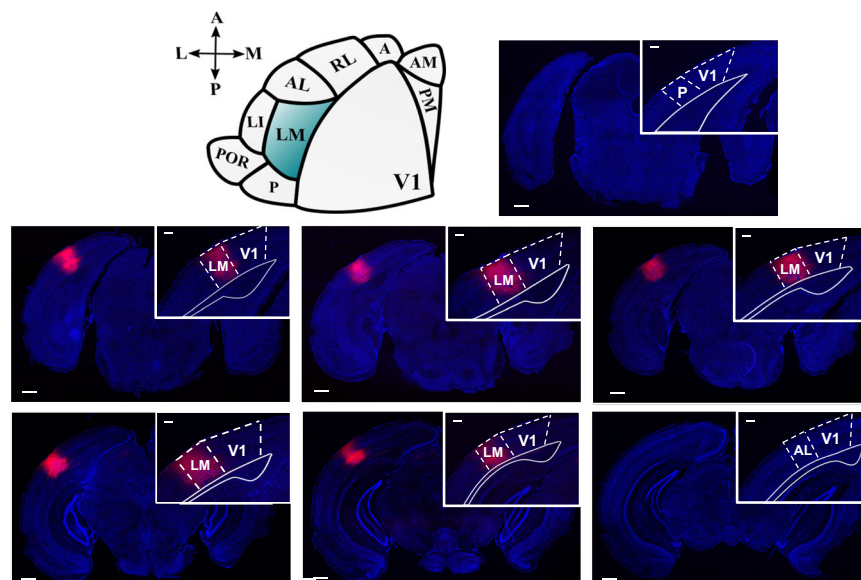

Fig. 4 | mCherry expression and HVAs. Representation of the HVAs along the postero (P) anterior (A) and latero (L) medial (M) axes. The anatomical transition between the LM and AL cortex is considered the physiological border between the ventral and dorsal visual streams. mCherry expression was entirely confined into the ventral stream. No fluorescence could be detected within AL borders. Scale bar 500 μm; inset 200 μm. To ensure the correct localization of the injections, three random slices for each animal were aligned to Allen Mouse Brain Atlas using QuickNII. Abbreviations for visual areas: V1, primary visual cortex; A, anterior; AL, anterolateral; AM, anteromedial; LI, laterointermediate; LM, lateromedial; P, posterior; PM, posteromedial; POR, postrhinal; RL, rostrolateral.
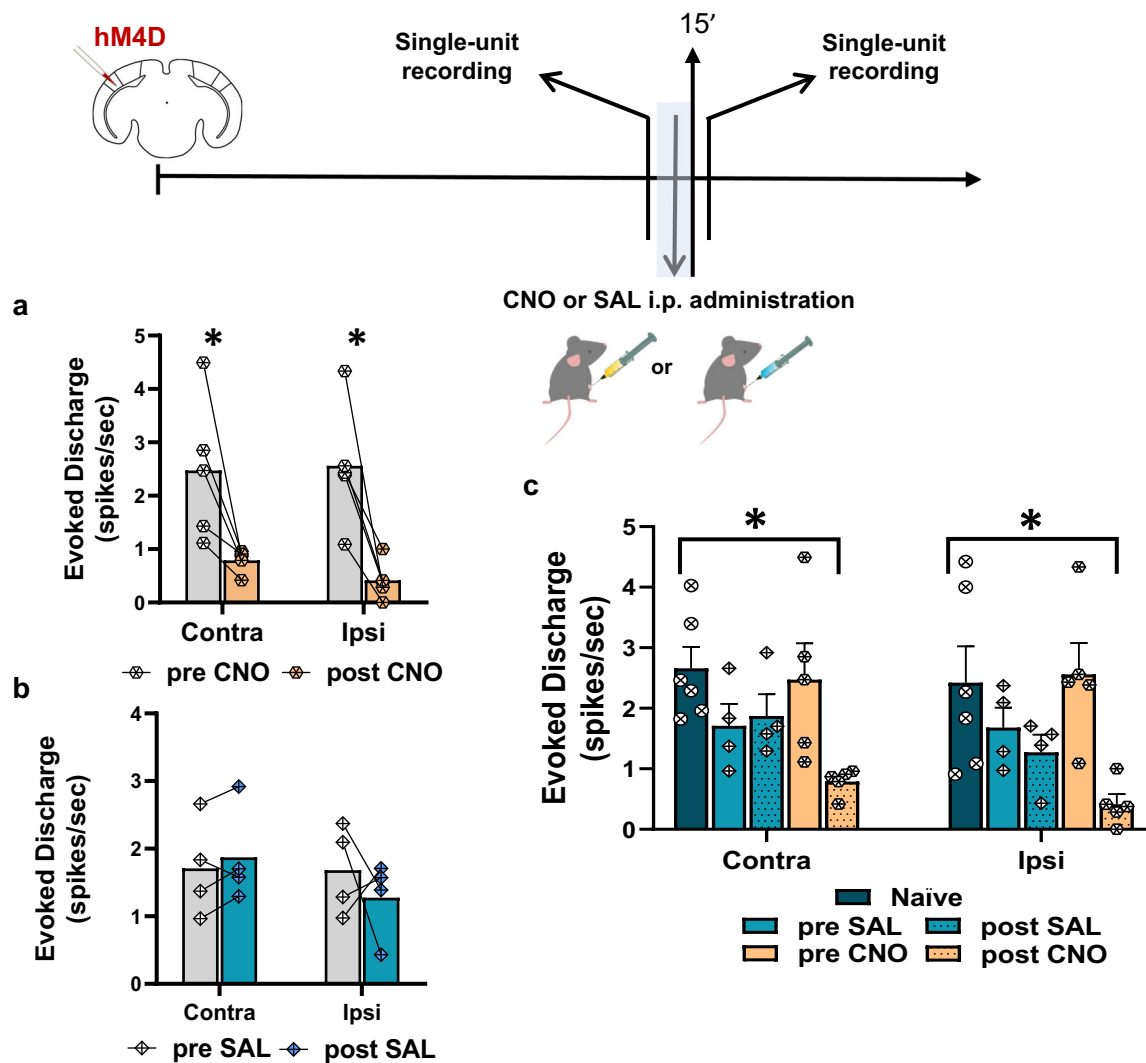
Fig. 5 | Electrophysiological assessment of LM inhibition. Single units were recorded around 400 μm of cortical depth in a group of injected mice before and 15 min after the i.p. injection of CNO or saline, keeping all the recording parameters fixed. **a** A significant decrease in LM activity was detected after CNO administration ($n = 5$, contralateral eye: paired t test, $p = 0.038$; ipsilateral eye: two-tailed paired t test, $p = 0.014$). **b** In contrast, no changes in LM activity were detected after saline administration in a separated group of injected mice ($n = 4$, contralateral eye:

paired t test, $p = 0.375$; ipsilateral eye: two-tailed paired t test, $p = 0.516$). **c** After CNO administration, only the LM activity recorded from post-CNO mice was significantly different from that of naïve mice ($n = 6$, One-way ANOVA, contralateral eye: $p = 0.02$ and ipsilateral eye: $p = 0.031$). Single dots were obtained averaging all the recorded single units in each animal. *Statistical significance. Error bars, s.e.m. Source data are provided as a Source Data file.

activation, we also measured behavioral visual acuity (VA) after LM inactivation. VA was assessed through the Prusky water maze task[61], testing the ability of injected mice to distinguish a visual grating from an homogeneous gray stimulus. Two weeks after a bilateral injection of hM4D, a separate group of mice ($n = 8$) was first trained with a low SF and then tested for the capability to distinguish higher SFs 30 min after i.p. administration of saline. At the end of this first part of the procedure, the averaged VA was of 0.514 ± 0.005 c/deg. Then, mice were retested in the same task 30 min after i.p. administration of CNO. The VA measured in the same group of mice after CNO administration was 0.516 ± 0.005 c/deg. Thus, no VA impairment could be found when LM activity was suppressed (paired t test, DF = 7, $t = -0.678$, $p = 0.519$, Fig. 7).

LM activity is required for vPL retention

We then asked whether the vPL impairment caused by LM inactivation could be reversed by a treatment shift in which CNO was replaced by saline administration, and vice versa, whether the intact vPL abilities displayed by mice originally treated with saline might be impaired by a treatment shift in which saline was replaced by CNO administration. To

this purpose, CNO and SAL mice were subjected to an experiment of administration shift (AS). When the animals reached their perceptual plateau, CNO mice were subjected to i.p. administration of saline, and then to additional vPL practice (CNO_SAL mice); vice versa, after reaching their perceptual plateau, SAL mice were subjected to administration of CNO, and then to additional vPL practice (SAL_CNO mice) (Fig. 8). Both groups of animals were asked to perform additional vPL, starting 30 min after the first administration of the new treatment. Injections were repeated 30 min before each vPL session, as previously described for CNO and SAL mice.

CNO_SAL mice displayed a marked improvement in their vPL performance. While, immediately after AS, the MDT of CNO_SAL mice was not significantly different from that achieved before AS (paired t test, DF = 7, $t = 2.004$, $p = 0.085$, Fig. 8a), they eventually reached a new MDT (0.048 ± 0.003 c/deg) that was significantly lower than that reached before AS (paired t test, DF = 7, $t = 4.379$, $p = 0.003$, Fig. 8a), and no longer different with respect to that achieved by both vPL and SAL mice (One-way ANOVA on ranks, DF = 2, $p = 0.587$). On the other hand, SAL_CNO mice were only able
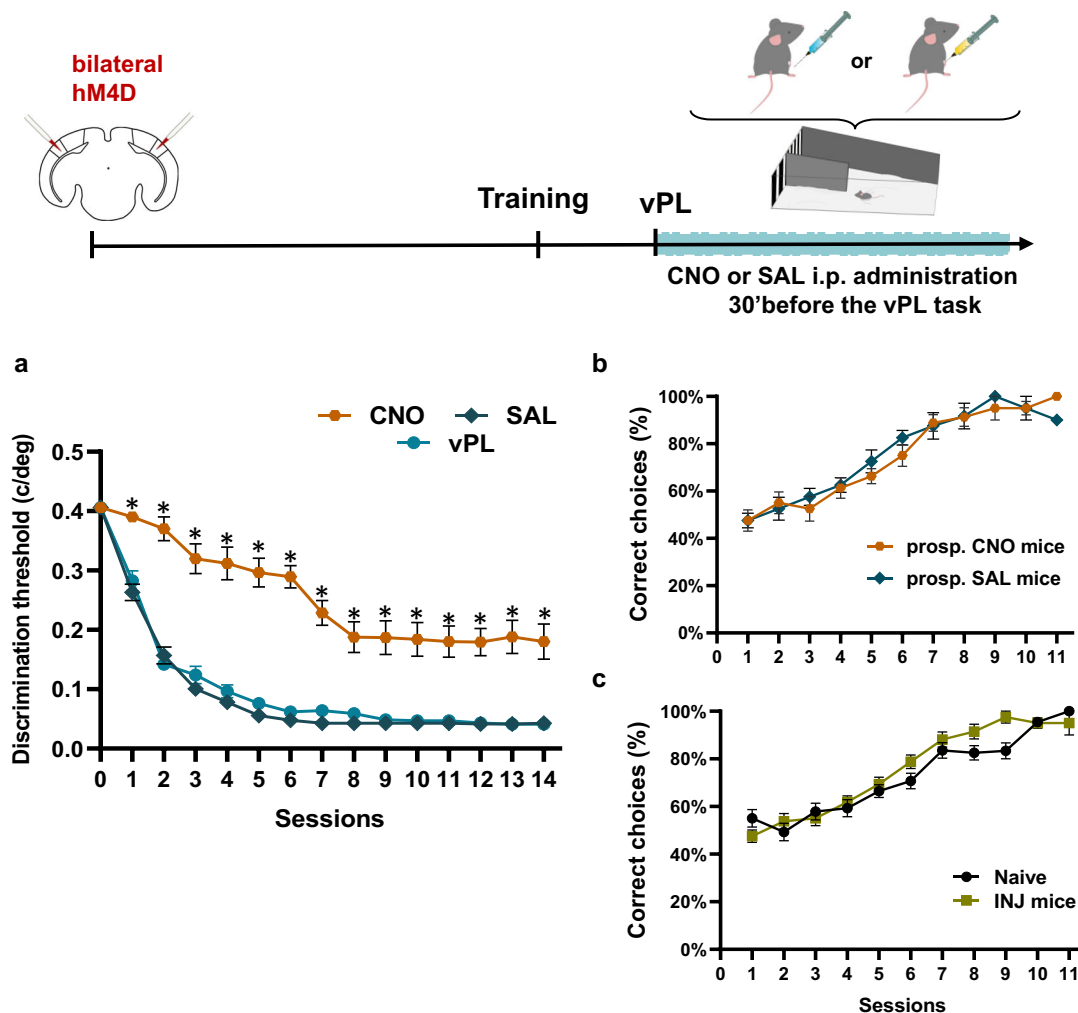
Fig. 6 | LM inhibition impairs vPL. A group of injected mice was subjected to the vPL task 30 min after the i.p. administration of either CNO (CNO mice) or saline (SAL mice) before each session. Their vPL curves were then compared to the performance of naïve mice previously subjected to the same perceptual task (vPL mice). **a** CNO mice showed a strong vPL impairment during the perceptual task compared to SAL mice ($n = 8$ CNO and $n = 8$ SAL, Two-way RM ANOVA on ranks, Holm–Sidak method, $p < 0.001$). Compared to vPL and SAL mice, the perceptual performance of CNO mice was altered throughout the vPL task ($n = 7$ vPL, Two-way RM ANOVA on ranks, Holm–Sidak method, $p < 0.001$). CNO mice indeed displayed a different vPL progression and achieved a higher MDT. **b** The discrimination abilities of CNO and SAL mice were different during the incremental phase of the vPL task, but not during the training phase ($n = 8$ prosp. CNO and $n = 8$ prosp. SAL, Two-way RM ANOVA, Holm–Sidak method, $p = 0.757$). **c** To evaluate the effects of the surgical procedure on learning capability, the learning performance during the training phase of injected mice ($n = 16$, CNO and SAL mice pooled together) was compared to that of naïve mice ($n = 14$, vPL and FS mice pooled together). No difference could be found between these two groups of animals (Two-way RM ANOVA, Holm–Sidak method, $p = 0.200$). *Statistical significance. Error bars, s.e.m. Source data are provided as a Source Data file.

to discriminate the easiest set of stimuli of our vPL task immediately after AS (paired t test, test on ranks, $p = 0.008$, Fig. 8b). When additional vPL was applied, SAL_CNO mice reached a new MDT (0.319 ± 0.026 c/deg) that was significantly higher than that achieved before AS (paired t test on ranks, $p = 0.008$, Fig. 8b) and then that achieved by vPL mice (t test, DF = 13, $t = -8.702$, $p < 0.001$).

When LM activity was suppressed, the vPL performance of CNO, but not that of SAL mice, was significantly different compared to the performance of vPL mice- naïve animals subjected to the same vPL task (One-way ANOVA on ranks, Dunn's Method, p < 0.001, Supplementary Fig. 4a). Instead, the MDT of SAL mice treated with CNO (SAL_CNO) but not that of CNO mice treated with SAL (CNO_SAL) was significantly different compared to the performance of vPL mice (One-way ANOVA on ranks, Dunn's Method, $p < 0.001$, Supplementary Fig. 4b). Notably, we found that major perceptual impairments can be induced suppressing LM activity after vPL acquisition (SAL_CNO mice). The MDT achieved by SAL_CNO mice (MDT = 0.319 ± 0.026 c/deg) was indeed significantly higher than the MDT achieved by CNO mice, i.e. those

animals subjected to LM suppression from the very first vPL session (MDT = 0.180 ± 0.029 c/deg) (t test on ranks, $p = 0.021$, Supplementary Fig. 4c).

Taken together, these results show that interfering with the neuronal activity of LM leads to a marked impairment not only of vPL acquisition but also of its retention (Supplementary Fig. 5a).

The role of top-down projections in vPL

To gain conclusive insights into the role played by top-down LM to V1 projections in vPL, we spatially confined our chemogenetic suppression to those secondary visual neurons directly projecting into V1 (LM > V1 projections) in a separate group of animals. To suppress LM > V1 projections, we induced the expression of a Cre-dependent hM4D delivered into LM by injecting retro-Cre within V1 borders. Through this double-injection strategy, we were able to selectively label and suppress only those LM neurons sending top-down projections to V1. As previously described for the chemogenetic suppression of LM, mice were subjected to the vPL task
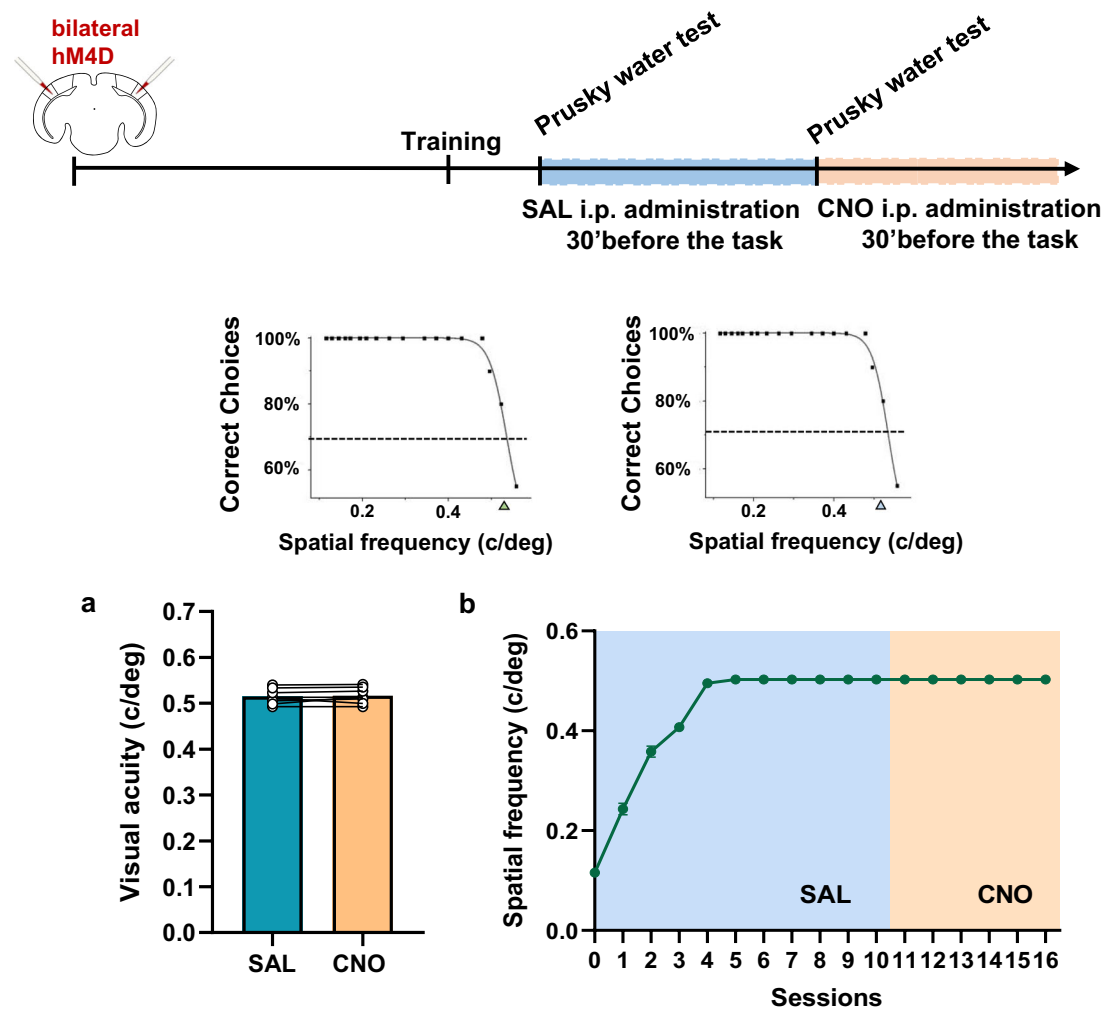
Fig. 7 | Assessment of visual acuity in a group of injected mice. Visual acuity (VA) was measured in a group of injected mice to rule out any potential visual impairments caused by LM inhibition. VA was measured using the water maze test. Examples of sigmoidal extrapolations of psychometric curves used to calculate VA are reported on the top panel. **a** No significant differences could be found in the VAs measured before and after the chemogenetic inhibition of LM ($n = 8$, two-tailed paired t test, $p = 0.519$). **b** Progression in the water maze task after an i.p. administration of saline (light blue panel) or CNO (orange panel). *Statistical significance. Error bars, s.e.m. Source data are provided as a Source Data file.

30 min after an i.p. administration of CNO (PRJ CNO mice, $n = 7$). A significant deficit in vPL was found when LM > V1 projections where selectively suppressed, with PRJ CNO mice reaching a mean MDT of 0.235 ± 0.031 c/deg (Fig. 9a). The final perceptual plateau reached by PRJ CNO mice was not different from that previously reported for CNO mice (Two-way RM ANOVA on ranks, Holm–Sidak method, overall treatment, CNO mice vs PRJ CNO mice $p = 0.333$; SAL mice vs PRJ CNO $p < 0.001$; CNO mice vs SAL mice $p < 0.001$, Fig. 9a).

We then tested whether the vPL deficit exhibited by PRJ mice could be rescued by a shift to saline administration, as previously observed in CNO mice. When PRJ CNO mice achieved their perceptual plateau, they were subjected to additional vPL practice 30 min after a saline i.p. administration (PRJ CNO_SAL mice). When LM > V1 projections were released from the chemogenetic suppression, PRJ CNO_SAL mice showed an improvement in their performance (0.235 ± 0.031 c/deg vs 0.188 ± 0.039 c/deg; paired t test, $t = 2.576$, DF = 6, $p = 0.042$, Fig. 9b), continuing to improve until they achieved a new MDT (0.043 ± 0.006 c/deg, paired t test, $t = 6.606$, DF = 6, $p < 0.001$, Fig. 9b).

Similarly to what was observed when the global LM activity was suppressed, we found that PRJ CNO mice achieved a vPL plateau statistically different from SAL mice, but not from CNO mice (One-way ANOVA on ranks, $p < 0.001$, Fig. 9c). However, when the activity of LM > V1 projections was rescued, PRJ CNO_SAL mice achieved a new perceptual plateau statistically different from SAL_CNO mice, but not from CNO_SAL mice (One-way ANOVA on ranks, $p < 0.001$, Fig. 9d).

Overall, these results strongly show a key role for top-down projections that re-enter V1 from LM in the acquisition of vPL (Supplementary Fig. 5b).

Discussion

Top-down processing is increasingly recognized as crucially involved in visual perception[54,55]. Previous results have shown that vPL improvements require the elaboration of visual signals by higher-order areas[33,43]. However, the effects on vPL of a precise spatiotemporal control of higher order areas was still missing, along with a chronic interference of higher-order activity throughout a vPL task. In our study, we provide evidence that neuronal activity in a higher-order visual area belonging to the ventral stream is crucial for both the acquisition and retention of vPL.

To analyze this hypothesis, we developed a mouse model of vPL adapting a visual discrimination task[22,46] previously studied in humans
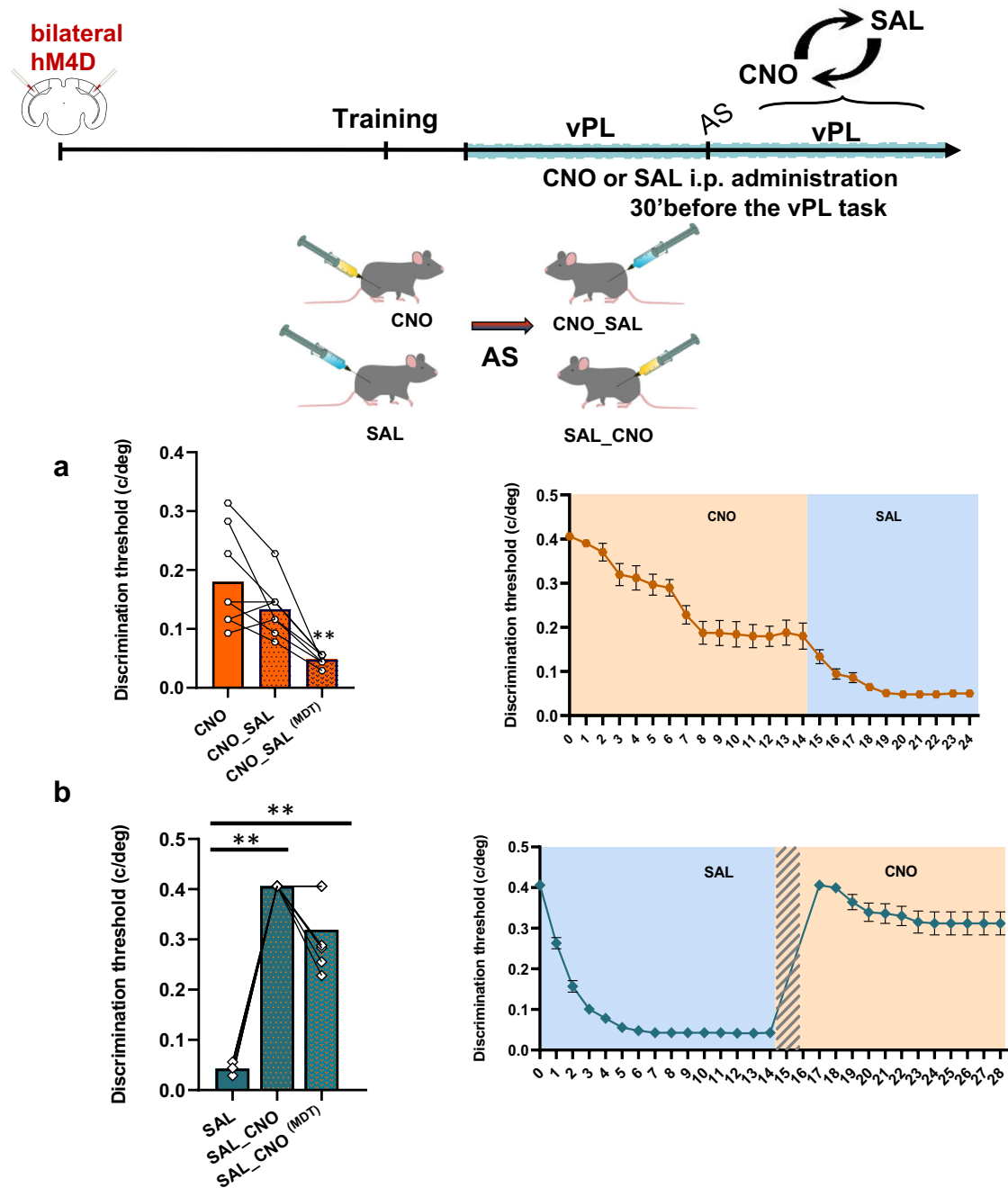
Fig. 8 | Administration shift. a Immediately after the administration shift, no changes could be detected in the performance of CNO_SAL mice ($n = 8$, two-tailed paired t test, $p = 0.085$). After additional vPL practice, CNO_SAL mice showed a significant improvement in their perceptual performance (two-tailed paired t test, $p = 0.003$). Right panel: vPL progression of CNO mice before and after the administration paradigm. When LM was released from chemogenetic inhibition, the group of former CNO mice (now CNO_SAL mice) underwent a progressive vPL improvement. **b** Immediately after the administration shift, SAL_CNO mice could only discriminate a significantly higher DT ($n = 8$, two-tailed paired t test on ranks, $p = 0.008$). Even when additional vPL practice was applied, SAL_CNO mice were still impaired in performing the vPL task (two-tailed paired t test on ranks, $p = 0.008$). Right panel: vPL progression of SAL mice before and after the administration paradigm. A marked perceptual impairment was detected in the vPL performance of the former SAL mice (now SAL_CNO mice) when LM activity was suppressed, with mice being completely unable to perform the vPL task for two consecutive sessions (gray bars). *Statistical significance. Error bars, s.e.m. Source data are provided as a Source Data file.

and rats[15,16,62–64]. We found that a robust and reliable vPL process can also be induced in adult mice, with trained animals reaching a steady perceptual plateau after few training sessions. We report that the observed vPL improvements do not transfer to orthogonal stimuli. Consistently, several studies proved that perceptual improvements in visual discrimination return to baseline levels when the trained stimuli were altered. Specifically, we previously demonstrated that the effects

of practice in discriminating SF difference do not transfer when the visual stimuli are rotated by 90°[15,46], but only when the visual gratings are rotated by an angle of less than 45° from the orientation used in vPL trials[15]. Our results suggest that perceptual improvements engage lower stages of visual cortical processing, where neurons have relatively small receptive fields and are selective for stimulus orientations[26]. In contrast, rule learning seems to rely on higher stages
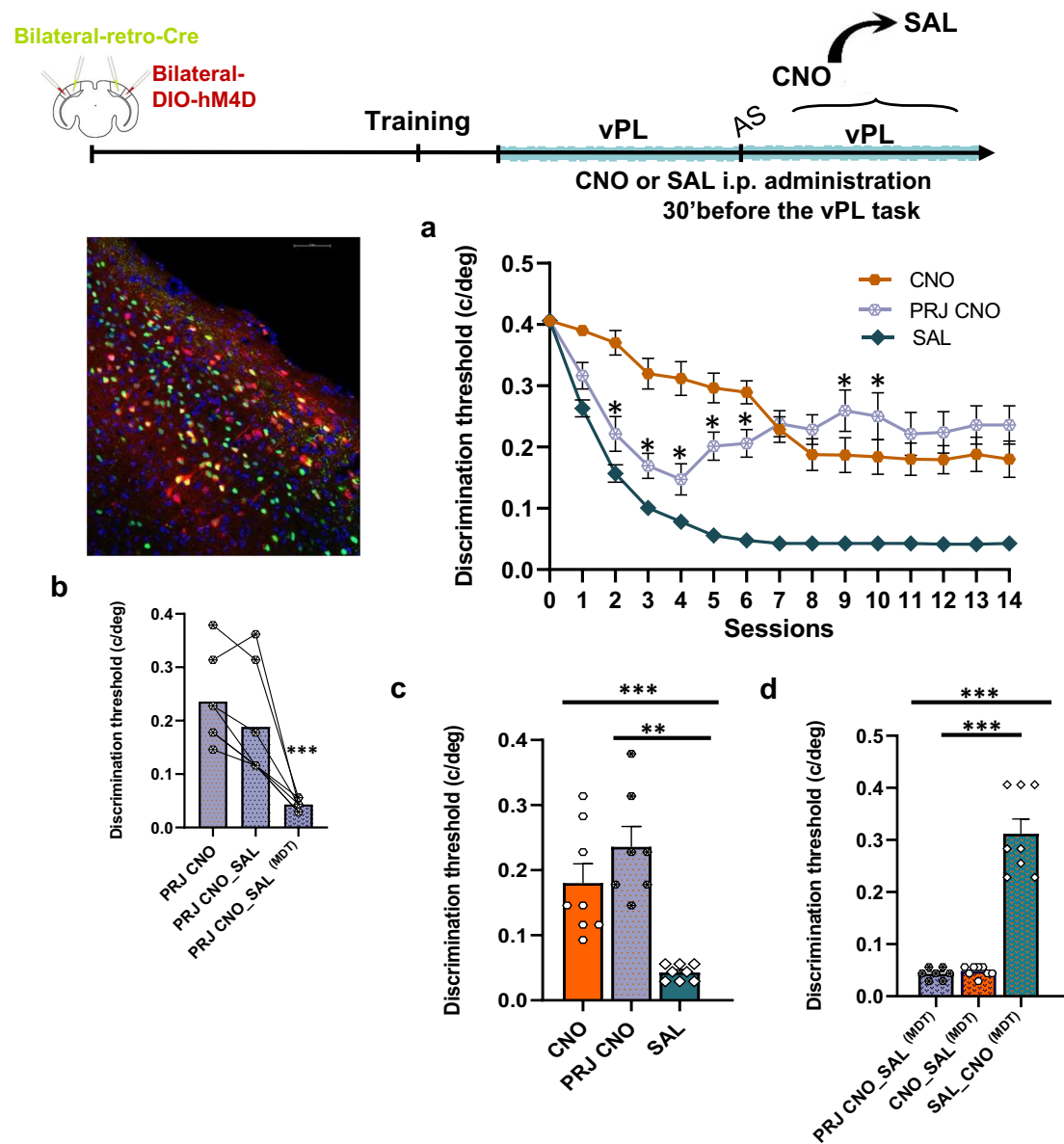
Fig. 9 | Selective suppression of LM > V1 top-down projections impairs vPL. In a separate group of mice, we specifically targeted chemogenetic suppression to the top-down projections re-entering V1 from LM. These animals were first subjected to the vPL task 30 min after an i.p. administration of CNO (PRJ CNO mice). **a)** After the first session, PRJ CNO mice showed an initial vPL progression statistically different from CNO and SAL mice, and then displayed a robust vPL deficit ($n = 8$, Two-way RM ANOVA on ranks, Holm-Sidak method, treatment: $p < 0.001$). **b** When the perceptual plateau was achieved, PRJ CNO mice were subjected to the administration shift paradigm, as previously described for CNO and SAL mice. Immediately after saline administration, the vPL performance of PRJ CNO_SAL significantly improved

(two-tailed paired t test, $p = 0.084$). When additional vPL practice was applied, a further improvement in the vPL performance was detected (two-tailed paired t test, $p < 0.001$). **c** When administered with CNO, PRJ CNO mice achieved an MDT different from SAL but not CNO mice ($n = 8$ per group, One-way ANOVA on ranks, $p < 0.001$), displaying a clear vPL impairment. **d** In contrast, PRJ CNO_SAL achieved an MDT different from SAL_CNO but not CNO_SAL mice ($n = 8$ per group, One-way ANOVA on ranks, $p < 0.001$). Immunohistochemistry labeling: red-mCherry, green-eGFP, yellow-merge, blue-Hoechst. *Statistical significance. Error bars, s.e.m. Source data are provided as a Source Data file.

of visual cortical processing, since the learned ability to perform an easy discrimination task (FS training) generalizes across orthogonal orientations.

The observed high specificity for trained orientation supports a prime role of V1 in vPL. Previous studies have accordingly reported that perceptual improvement can return to baseline levels changing the stimulus features used during vPL practice[20,23,65]. V1 recruitment in vPL is supported not only by behavioral observations, but also by electrophysiological and imaging studies[28–34]. vPL practice is indeed associated with structural changes in V1 circuitry[35,66]. In particular, we previously reported that vPL correlates with LTP occlusion within

V1[46]. However, the emergence of local plastic changes inside V1 circuitry was evident not only at the level of vertical connections conveying information from the lateral geniculate nucleus of the thalamus (bottom-up stream), but also at the level of horizontal connections, that can drive information from higher order areas (top-down processing)[46]. Consistently, plastic changes in response to vPL practice can also be found in higher stages of visual cortical processing[44,67,68]. The encoding and retrieval of internal computations regarding the external context, reward or prior vPL practice, could therefore rely on the activity of higher-order visual neurons.

With the specific aim of probing the role of top-down processing in vPL, we chemogenetically suppressed LM activity before each vPL session. We focused our work on LM based on previously obtained anatomical and physiological results. Primarily, the great majority of feedback projections entering V1 from HVAs sprout from LM[50]. LM is currently considered the gateway of the mouse ventral stream[51], a highly interconnected network of four lateral higher-order visual areas whose projections find their prime target in a cluster of ventral structures implicated in learning and memory processes[48]. Previous studies have shown that anatomical lesions to visual areas belonging to this pathway can severely impair perception and object identification[52,53,69]. Furthermore, anatomical evidence suggests that LM is the homologous of the primate V2 in the mouse visual system[47]. LM might therefore represent the first higher cortical stage in which visual associations start to emerge.

When LM activity was functionally disconnected from V1, CNO treated mice displayed vPL impairments in the task progression and in the achieved perceptual plateau. Strikingly, the observed learning impairment could be completely reversed releasing LM from the chemogenetic inhibition, a result that strongly suggests that LM is crucial for vPL acquisition. In a separate group of mice, LM activity was instead suppressed when the vPL task was already completed. Major vPL deficits can be induced under this experimental setting, with all trained mice being able to only distinguish the SF difference used in the training trials. Even after additional vPL practice, the acquired vPL performance in terms of discrimination threshold could no longer be restored while LM activity was suppressed. This suggests that LM is also required to retain vPL improvements.

We further analyzed the role of top-down LM > V1 projections in vPL. The selective inactivation of these re-entrant fiber led to a critical failure in the acquisition of vPL expertise. PRJ CNO mice displayed an equivalent vPL deficit in the perceptual plateau to what recorded when the entire LM activity was suppressed, although the initial progression in the vPL task does not overlap with the initial vPL performance of CNO mice. This difference suggests that the flow of information re-entering V1 from LM is crucially required to perceive small difference in the presented visual stimuli, i.e. when the spatial frequency difference between the stimuli is small. Another interpretation is that the initial difference could be ascribed to the total amount of LM > V1 projections that we were able to suppress with our chemogenetic selective approach. Either way, we found that both LM internal activity and top-down projection streaming from LM are crucially required for the acquisition of vPL expertise.

The results presented in this paper can be analyzed within the framework of computational models supporting the notion that vPL is accomplished by weight changes between higher and lower visual areas[70,71]. A classic computational model dealing with top-down integration in vPL is the reverse hierarchy theory (RHT)[72,73]. RHT postulates that vPL occurs in a reverse hierarchy order, with lower-level learning being guided by higher-order learning processes. In this model, perceptual expertise is therefore acquired through a learning cascade from prior higher-order representations, coding for easy-condition learning, to difficult-condition learning processed in lower-order levels, where external signals can be filtered at fine spatial resolution[74,75]. In contrast to this model, our data show that when V1 was functionally disconnected from LM, we detected a significant impairment in the more difficult-condition rather than in the easier-condition learning task: indeed, mice treated with CNO failed to complete the vPL task; in contrast, vPL performance of SAL_CNO mice fell to an easy-condition (training level) right after the administration shift. Our results might instead better fit the augmented Hebbian reweighting model of VPL. According to this model, vPL relies on task-specific changes in the strength of neuronal connections between lower-level and higher-level visual cortical representations. In this

scenario, perceptual expertise results from a process of network reweighting guided by higher-order visual areas that refines cortical readout by assigning different weight to task-relevant inputs[76–78]. We consistently proved that LM activity is required for vPL acquisition and retention with top-down projections specifically recruited in the more difficult-condition learning condition.

It is worth noticing that we can exclude the possibility that vPL impairments were due to nonspecific visual deficits. A separated group of CNO treated mice, indeed, was shown to display no detectable deficits in behavioral visual acuity with respect to naïve mice engaged in the same task[61]. Even though orientation tuned neurons are also present in subcortical regions (such as the superior colliculus)[79], it seems implausible that these subcortical pathways could account for the recorded visual acuity values, as the colliculus works at a lower discrimination resolution than the visual cortex.

Despite the critical function of LM, the possibility that other higher-order areas could have a role in vPL cannot be excluded and certainly deserves future investigation. Mouse V1 is indeed surrounded by at least nine retinotopically organized areas[36,47]. In particular, we cannot exclude a role in vPL played by other visual areas along the ventral streams. For example, several studies have demonstrated that the postrhinal cortex (POR) is required for contextual scene representation[80], encoding the association between a visual cue and the reward[81] and the internal representation linking objects to places[80].

Further studies are also needed to precisely uncover the mechanisms of the LM-to-V1 top-down interaction in vPL. According to anatomical studies, feedback projections from LM to V1 are mostly excitatory by nature[82,83]. Therefore, it is possible that V1 circuitry changes under the influence of top-down inputs that directly target selected primary visual neurons, probably recruiting the horizontal connections[1,84]. In parallel to a role for excitatory connections, recent studies support the notion of a not negligible role of the inhibitory system in top-down integration[85–87]. A prime role of the GABAergic system in vPL finds also support in biochemical assays showing a substantial reduction in the inhibitory tone after vPL practice[62]. Future studies might focus on the role of specific subclasses of interneurons in top-down processing[83].

In conclusion, the demonstration that top-down projections from LM play a key role in the learning process that leads to visual perceptual improvement is an essential step towards unraveling the neural networks responsible for the neural underpinnings of vPL.

Methods

Animal treatment

C57BL/6J (WT) mice of 2-3 months of age were used in this study, in accordance with the approved guidelines and regulations of Italian Ministry of Public Health. All experimental protocols were approved by the Italian Ministry of Public Health (Authorization n. 545/2023-PR). The experiments have been designed to minimize the number of animals used and their discomfort or distress. Animals were housed in a room with a temperature of 22 °C and a 12 h light/dark cycle; food and water were provided ad libitum.

Visual perceptual learning task

We used a modified version of the Prusky water maze task, displaying a set of visual stimuli per trial[46,61]. The apparatus consisted of a trapezoidal-shaped pool with two computer-controlled monitors (40 cm diagonal screen size) placed side-by-side at one edge of the pool. The pool (140 cm long, 55 cm high) was made of 6 mm Plexiglas, with one edge (80 cm) wider than the other one (25 cm). All the walls were finished on the inside with black paint to reduce reflection. The pool longitudinal axis was bisected by a midline divider (50 cm long) that, sitting between the monitors, extended from the wider edge into the pool. The divider was painted black to

reduce reflection within the pool. The length of the divider set the animal decision point, from which the spatial frequency (SF) of the stimuli was calculated by the same computer software generating the visual stimuli. The decision point was the closest an animal could get to the monitors without choosing a side entering one of the two arms set by the divider. Visual stimuli were presented by the monitors through two glass windows carved on the wider pool edge. Stimuli consisted of visual gratings at the same luminance (40.06 cd/m²) and contrast (100%). A set of two visual gratings was presented per each trial. The spatial frequency (SF) of one grating was kept at 0.116 c/deg throughout the behavioral task (reference grating). The SF of the other grating was changed according to task phase or experimental conditions (test grating). A custom-made software was used to decide which monitors displayed the reference grating, alternating the position of the test and reference grating in a pseudorandom schedule where no more than three trials on the same side were allowed. The pool was filled with tepid (25 °C) water to a depth of 15 cm. A submerged platform was placed below the monitor displaying the reference grating. Between trials, the platform position was manually changed when the reference grating was displayed on the opposite side. White paint was added to the water preventing the animals from directly spot the platform through the water. Mice were released into the pool facing the monitors and were allowed to find the platform under the reference grating. A trial was recorded as correct when mice reached the platform entering directly the side displaying the reference grating. On all trials, mice were required to swim until they found the platform. A group of mice was first trained to distinguish a test grating of 0.522 c/deg from the reference grating, until they achieved a performance level of at least 80% of accuracy in three subsequent sessions (training phase). Once this criterion was reached, for a first group of mice (vPL mice) the vPL task was started by gradually reducing the SF of the test grating. If the animal made a correct choice, the SF of the test grating was decreased by one step and another trial was executed. This procedure continued until an error was made. Once an error occurred, the SF was increased by one step and another block of trials was run. After trials covering approximately half of the animal's projected threshold were completed, the minimum number of trials in a block was increased to four. For the last three SFs of the test grating, the required performance to decrease the SF was always ≥70% correct choices. A mean discrimination threshold (DT) was measured per each session until the mouse performance reached a steady plateau (minimum discrimination threshold, MDT). DT was defined as the smallest SF difference between the two stimuli at which the animal performance was above the criterion of at least 70% of correct choices. Mean DT was obtained averaging the DT that each mouse achieved within a session. In parallel, a different group of control mice (first-step (FS) mice) was allowed to only discriminate the reference grating from a test grating whose SF was always maintained at the starting value of 0.522 c/deg. FS mice were matched to vPL mice in terms of overall swim time and training sessions in the water tank. When the performance plateau was reached, an experiment of stimulus orientation shift was performed: the orientation of the two gratings was rotated by 90°. For each mouse, the vPL task restarted from the final DT perceived before the orientation shift and new trials were applied to measure the MDT for horizontal gratings.

In vivo electrophysiology

Electrophysiological recordings were performed as previously described[88]. Mice were anesthetized with an i.p. injection of urethane (0.7 g/kg, 20% in saline; Sigma-Aldrich) and placed on a stereotaxic frame, with the body temperature maintained at 37 °C, and were also ventilated through an oxygen mask. During surgery, the eyes were protected by applying a dexamethasone-based ointment (Tobradex, tobramycin 0.3% and dexamethasone 0.1%). A craniotomy was performed over the lateromedial visual cortex (3.6–4.1 mm lateral to lambda), leaving the dura mater intact. An electrode (2 × 2-tet-3 mm-150–150-121-A16-15, Neuronexus Technologies) was slowly lowered into LM cortex to record local field potentials and single-unit activity. Signals were acquired using a 16 channels Neuralynx device and data analysis was performed using custom MATLAB software. Visual stimuli were generated in MATLAB using Psychophysics Toolbox extension and displayed, with gamma correction, on a monitor (Sony Trinitron G500, 60 Hz refresh rate, 32 cd m − 2 mean luminance) placed 20 cm in front of the animal.

For visual evoked potentials (VEPs), the extracellular signal was filtered from 0.1 to 275 Hz and sampled at 20 kHz. VEPs in response to sinusoidal wave patterns with a spatial frequency of 0.06 c/deg and abrupt phase inversion (1 Hz temporal period), were evaluated in the time domain by measuring the peak-to-baseline amplitude and latency. VEPs were acquired using the responses coming only from the tetrode in the upright position inside the inserted probe (responses from the four contact points were averaged together), at 200 μm of cortical depth. Computer controlled mechanical shutters were used to alternatively close the two eyes. The presented spatial frequencies and contrast percentages were within the range classically used in the mouse model, in agreement with a vast literature in this field[56,57,61]. Visual acuity and contrast threshold were then obtained by extrapolation to zero amplitude of the linear regression through the data points in a curve where VEP amplitude was plotted against log spatial frequency or contrast percentage, respectively.

For single-unit recordings, the extracellular signal was filtered from 0.6 to 9 kHz and sampled at 30.3 kHz. To improve single-unit isolation, recordings from groups of four neighboring sites (tetrode) were linked, so that each spike was composed by four waveforms. Data was loaded on the Offline Sorter software (Plexon), and a principal component analysis was performed to score spikes with a high degree of similarity in a 3D feature space. Waveforms from each electrode of the tetrodes were processed together to improve isolation. Clusters were progressively defined using convex hulls and then recalculating principal component analysis. Quality of separation was determined based on the following criteria: (1) during manual clusterization with convex hulls, raw waveforms in the clusters were visually inspected to check the uniformity of single waveforms; (2) clusters contained <0.1% of spikes within a 1.0 ms interspike interval; (3) auto- and cross-correlograms of the clusters were also inspected to reveal if the cluster contained more than a single unit or if several clusters contained spikes of the same unit; and (4) the peak amplitude of a unit remained stable over the entire recording session. Drifting sinusoidal gratings were used as visual stimuli (1.5 s duration, temporal frequency of 2 Hz, 12 different orientations with a step of 30°, 6 spatial frequencies: 0.01, 0.02, 0.04, 0.08, 0.16 and 0.32 c/deg). Stimulation was repeated five times per eye, with stimulus conditions randomly interleaved, and two gray blank conditions (mean luminance) were included in all stimuli sets to estimate the spontaneous firing rate. The average spontaneous rate for each unit was calculated by averaging the rate over all blank condition presentations. Responses at each orientation and spatial frequency were calculated by averaging the spike rate during the 1.5 s presentation and subtracting the spontaneous rate. The preferred stimulus was determined by finding the combination of spatial frequency and orientation that maximize the response, independently for each eye. Orientation tuning curves were constructed for the spatial frequency that gave maximal response at this orientation. Given this fixed preferred orientation (OPref), the tuning curve was fitted as the sum of two Gaussians centered on OPref and OPref + π, of different amplitudes but equal width, with a constant baseline. From this fit, we calculated an orientation selectivity index (OSI) representing the ratio

of the tuned versus untuned components of the response, and the width of the tuned component. OSI was calculated as follows: (respOPrefresp - OOrtho)/(respOPref + respOOrtho), where resp is the maximal response evoked by visual stimulation and OOrtho is the orientation orthogonal to the preferred one. Tuning width is the half-width at half-maximum of the principal Gaussian. In addition, a direction selectivity index (DSI) was calculated as follows: (respOPref-respOOppo)/(respPref + respOppo).

To assess ocular dominance (OD), sorted units were clustered in OD classes. OD classes were evaluated based on the ratio of contralateral to ipsilateral peak response. More specifically, neurons in ocular dominance class 1 were driven only by stimulation of the contralateral eye; neurons in ocular dominance classes 2 (ratio of contralateral to ipsilateral peak response, ≥2) and 3 (ratio of contralateral to ipsilateral peak response, between 1.2 and 2) were binocular and preferentially driven by the contralateral eye; neurons in ocular dominance class 4 were equally driven by the two eyes (ratio of contralateral to ipsilateral peak response, between 0.83 and 1.2); neurons in ocular dominance classes 5 (ratio of contralateral to ipsilateral peak response, between 0.5 and 0.83) and 6 (ratio of contralateral to ipsilateral peak response, ≤0.5) were binocular and preferentially driven by the ipsilateral eye; and neurons in ocular dominance class 7 were driven only by the ipsilateral eye.

Intracortical AAV injection in LM

Adult mice ($P > 60$) were anesthetized with isoflurane and mounted on a stereotaxic apparatus. An incision was made on the scalp, the skin above the skull was retracted and a hole was drilled into the skull over the LM (3.6 mm lateral to lambda) or V1 (2.8 mm lateral to lambda). Viral injections were performed using a 10 µL Hamilton syringe connected to a nanoliter syringe pump (Kd Scienti, speed 0.05 µL/min). To suppress LM activity, AAV8-hSyn-HA-hM4D(Gi)-mCherry (a gift from Bryan Roth (Addgene viral prep #50475-AAV8); http://n2t.net/addgene:50475; RRID: Addgene_50475), was delivered into LM. To specifically target top-down projections, AAV8-hSyn-DIO-hM4D(Gi)-mCherry (a gift from Bryan Roth (Addgene viral prep #44362-AAV8); http://n2t.net/addgene:44362; RRID: Addgene_44362) was delivered into LM and retro-pENN-AAV-hSyn-HI-eGFP-Cre (a gift from James M. Wilson (Addgene viral prep #105540-AAVrg; http://n2t.net/addgene:105540; RRID: Addgene_105540) into V1. Virus injections were made inserting a single syringe at two different cortical depths (220 and 450 µm below the pial surface) into LM (200 nL per injection site). All the injections were performed over a period of 4 min/per cortical depth, starting from the lowest site and then withdrawing the syringe to the upper site within the same insertion point. After each injection, the pipette was left in place for 2 more min and then gently withdrawn. For vPL experiments and VA assessment, mice were bilaterally injected. The scalp was then sutured, and an antibacterial pomade was applied along the sutures. During surgery, body temperature was maintained using feedback regulated heating pad. Mice were carefully monitored in the following days for recovery and engaged into experimental protocols 2 weeks after injection. To probe AAV expression, mice were perfused intracardially with PBS followed by 4% paraformaldehyde (PFA) in phosphate buffer. Brains were post-fixed overnight at 4 °C and then impregnated with 30% sucrose in phosphate buffer. Coronal brain sections (50 µm) were cut on a freezing microtome and collected in PBS. All reactions were performed on free-floating sections. After a washing step with PBS-T (PBS with 0.3% Triton), sections were incubated for 10 min at RT in Hoechst and mounted on glass slides and covered with VectaShield mounting medium. Fluorescence was acquired on a fluorescent microscope empowered with an Apotome 2.0 slit. To ensure the correct localization of the injections, three random slices for each animal were aligned to Allen Mouse Brain Atlas (https://atlas.brain-map.org/) using QuickNII (https://doi.org/10.1371/journal.pone.0216796) and inspected.

Chemogenetic experiments

For all chemogenetic experiments, CNO (Tocris Bioscience, Cat. No. 4936) was dissolved in sterile 0.9% NaCl, which was administered as vehicle.

Electrophysiological assessment of LM chemogenetic inactivation. To assess the chemogenetic suppression of LM, single units were recorded from a separate group of injected mice as previously described. The probe was lowered of 400 µm and single-unit responses were recorded before and 15 minutes after i.p. CNO administration (2 mg/kg) without changing the recording parameters. As control, a group of injected mice was instead recorded before and 15 minutes after i.p. saline administration (2 mg/kg). The electrical responses were compared to single units sorted from naïve animals at the same cortical depth.

Visual perceptual learning. Two weeks after surgery, a group of injected mice was subjected to the vPL task previously described. Once the 80% criterion was reached, mice were subjected to the incremental phase of the vPL task 30 min after an i.p. administration of CNO (2 mg/kg, CNO mice) or saline (2 mg/kg, SAL mice). Sessions were interleaved by a 4-hour gap to minimize animal discomfort and stress. When the performance plateau was reached, an experiment of administration shift was performed, i.e., CNO mice were subjected to i.p. administration of saline (CNO_SAL mice), and vice versa, SAL mice were subjected to i.p. administration of CNO (SAL_CNO mice). To assess the role of top-down projections, a different group of animals (PRJ mice) was subjected to the vPL task two weeks after the selective expression of inhibitory DREADDs in LM neurons projecting to V1. PRJ mice were asked to perform the vPL task 30 minutes after an i.p. administration of CNO (2 mg/kg, PRJ CNO mice). When the performance plateau was reached, PRJ CNO mice were administered with saline (2 mg/kg, PRJ CNO_SAL mice) 30 min before vPL. For each tested group (CNO_SAL, SAL_CNO, PRJ CNO_SAL), the vPL task restarted from the last DT perceived before the administration shift and additional vPL training was then applied to measure MDT under these new experimental conditions.

Behavioral assessment of visual acuity. VA was measured in a separated group of injected mice two weeks after AAV intracortical injection. VA was assessed through the behavioral method of the Prusky water maze task[61] employing the same arena described for the vPL task. To assess VA, mice were required to distinguish a visual grating from a homogenous gray rather than a set of two visual gratings. In this experimental setting, the submerged platform was always placed below the grating displayed by one of the two monitors. A trial was recorded as incorrect when mice entered directly the pool side displaying the gray stimulus. Mice were first trained to distinguish a low (0.116 c/deg) SF vertical grating. Once animal performance achieved a level of at least 80% of accuracy in three subsequent sessions (training phase), VA limit was estimated by increasing the SF of the grating (test phase). VA has been taken as the SF corresponding to 70% of correct choices on the sigmoidal function fitting the psychometric function. Mice were subjected to training phase sessions 30 minutes after i.p. saline administration (2 mg/kg). Then, starting from the last SF at which animal performance was ≥70% of correct choices, mice were subjected to the task 30 minutes after i.p. CNO administration (2 mg/kg), and VA was reassessed.

Statistical analysis

Statistical analysis was done using SigmaStat Software. Data were tested for normality before running statistical tests; parametric tests were run on normally distributed data and, in case normality test failed, non-parametric tests were performed as appropriate. Differences between two independent groups were assessed with

a two-tailed *t* test; differences between two dependent groups were assessed with a two-tailed paired *t* test. One-way ANOVA, One-way RM ANOVA, and Two-way RM ANOVA were used to compare normally distributed data belonging to more groups. One-way ANOVA or Two-way on ranks were performed to compare not normally distributed data belonging to more than two groups. The level of significance was $p < 0.05$, unless otherwise specified. The size of biological replicates is indicated by the n numbers in the various experimental sections.

Reporting summary
Further information on research design is available in the Nature Portfolio Reporting Summary linked to this article.

Data availability
All data supporting the findings of this study are available in the paper and its supplementary information files. Source data are provided with this paper.

Code availability
MatLab Code available upon request.

References
1. Gilbert, C. D. & Li, W. Top-down influences on visual processing. *Nat. Rev. Neurosci.* **14**, 350–63 (2013).
2. Gilbert, C. D. & Sigman, M. Brain states: top-down influences in sensory processing. *Neuron* **54**, 677–696 (2007).
3. Sperry, R. W. Neural basis of the spontaneous optokinetic response produced by visual inversion. *J. Comp. Physiol. Psychol.* **43**, 482–489 (1950).
4. Sommer, M. A. & Wurtz, R. H. What the brain stem tells the frontal cortex. II. Role of the SC-MD-FEF pathway in corollary discharge. *J. Neurophysiol.* **91**, 1403–1423 (2004).
5. Makino, H. Top-down control: a unified principle of cortical learning. *Neurosci. Res.* **141**, 23–28 (2019).
6. Makino, H. & Komiyama, T. Learning enhances the relative impact of top-down processing in the visual cortex. *Nat. Neurosci.* **18**, 1116–1122 (2015).
7. Gibson, E. J. *Principles of Perceptual Learning and Development.* (Appleton-Century-Crofts, 1969).
8. Goldstone, R. L. Perceptual learning. *Annu. Rev. Psychol.* **49**, 585–612 (1998).
9. Prettyman, A. Perceptual learning. *Wiley Interdiscip. Rev. Cogn. Sci.* **10**, e1489 (2019).
10. Schoups, A. A., Vogels, R. & Orban, G. A. Human perceptual learning in identifying the oblique orientation: retinotopy, orientation specificity and monocularity. *J. Physiol.* **483**, 797–810 (1995).
11. Matthews, N., Liu, Z., Geesaman, B. J. & Qian, N. Perceptual learning on orientation and direction discrimination. *Vis. Res.* **39**, 3692–3701 (1999).
12. Karni, A. & Sagi, D. Where practice makes perfect in texture discrimination: evidence for primary visual cortex plasticity. *Proc. Natl Acad. Sci.* **88**, 4966–4970 (1991).
13. De Valois, K. K. Spatial frequency adaptation can enhance contrast sensitivity. *Vis. Res* **17**, 1057–1065 (1977).
14. Mayer, M. J. Practice improves adults' sensitivity to diagonals. *Vis. Res.* **23**, 547–550 (1983).
15. Fiorentini, A. & Berardi, N. Learning in grating waveform discrimination: Specificity for orientation and spatial frequency. *Vis. Res.* **21**, 1149–1158 (1981).
16. Berardi, N. & Fiorentini, A. Interhemispheric transfer of visual information in humans: spatial characteristics. *J. Physiol.* **384**, 633–647 (1987).
17. Fine, I. & Jacobs, R. A. Perceptual learning for a pattern discrimination task. *Vis. Res.* **40**, 3209–3230 (2000).
18. Fendick, M. & Westheimer, G. Effects of practice and the separation of test targets on foveal and peripheral stereoacuity. *Vis. Res.* **23**, 145–150 (1983).
19. Gold, J., Bennett, P. J. & Sekuler, A. B. Signal but not noise changes with perceptual learning. *Nature* **402**, 176–178 (1999).
20. Ball, K. & Sekuler, R. Direction-specific improvement in motion discrimination. *Vis. Res.* **27**, 953–965 (1987).
21. Shiu, L.-P. & Pashler, H. Improvement in line orientation discrimination is retinally local but dependent on cognitive set. *Percept. Psychophys.* **52**, 582–588 (1992).
22. Fiorentini, A. & Berardi, N. Perceptual learning specific for orientation and spatial frequency. *Nature* **287**, 43–44 (1980).
23. Fahle, M. & Edelman, S. Long-term learning in vernier acuity: effects of stimulus orientation, range and of feedback. *Vis. Res.* **33**, 397–412 (1993).
24. McKee, S. P. & Westheimer, G. Improvement in vernier acuity with practice. *Percept. Psychophys.* **24**, 258–262 (1978).
25. Ramachandran, V. S. & Braddick, O. Orientation-specific learning in stereopsis. *Perception* **2**, 371–376 (1973).
26. Hubel, D. H. & Wiesel, T. N. Receptive fields of single neurones in the cat's striate cortex. *J. Physiol.* **148**, 574–591 (1959).
27. Dräger, U. C. Receptive fields of single cells and topography in mouse visual cortex. *J. Comp. Neurol.* **160**, 269–290 (1975).
28. Fahle, M. & Skrandies, W. An electrophysiological correlate of learning in motion perception. *Ger. J. Ophthalmol.* **3**, 427–432 (1994).
29. Bao, M., Yang, L., Rios, C., He, B. & Engel, S. A. Perceptual learning increases the strength of the earliest signals in visual cortex. *J. Neurosci.* **30**, 15080–15084 (2010).
30. Yotsumoto, Y., Watanabe, T. & Sasaki, Y. Different dynamics of performance and brain activation in the time course of perceptual learning. *Neuron* **57**, 827–833 (2008).
31. Jehee, J. F. M., Ling, S., Swisher, J. D., van Bergen, R. S. & Tong, F. Perceptual learning selectively refines orientation representations in early visual cortex. *J. Neurosci.* **32**, 16747–16753a (2012).
32. Crist, R. E., Li, W. & Gilbert, C. D. Learning to see: experience and attention in primary visual cortex. *Nat. Neurosci.* **4**, 519–525 (2001).
33. Li, W., Piëch, V. & Gilbert, C. D. Learning to link visual contours. *Neuron* **57**, 442–451 (2008).
34. Schoups, A., Vogels, R., Qian, N. & Orban, G. Practising orientation identification improves orientation coding in V1 neurons. *Nature* **412**, 549–553 (2001).
35. Yan, Y. et al. Perceptual training continuously refines neuronal population codes in primary visual cortex. *Nat. Neurosci.* **17**, 1380–1387 (2014).
36. Glickfeld, L. L. & Olsen, S. R. Higher-order areas of the mouse visual cortex. *Annu. Rev. Vis. Sci.* **3**, 251–273 (2017).
37. Crist, R. E., Kapadia, M. K., Westheimer, G. & Gilbert, C. D. Perceptual learning of spatial localization: specificity for orientation, position, and context. *J. Neurophysiol.* **78**, 2889–2894 (1997).
38. Li, W., Piëch, V. & Gilbert, C. D. Perceptual learning and top-down influences in primary visual cortex. *Nat. Neurosci.* **7**, 651–657 (2004).
39. Jordan, D. et al. Simultaneous electroencephalographic and functional magnetic resonance imaging indicate impaired cortical top-down processing in association with anesthetic-induced unconsciousness. *Anesthesiology* **119**, 1031–1042 (2013).
40. Ku, S.-W., Lee, U., Noh, G.-J., Jun, I.-G. & Mashour, G. A. Preferential inhibition of frontal-to-parietal feedback connectivity is a neurophysiologic correlate of general anesthesia in surgical patients. *PLoS ONE* **6**, e25155 (2011).
41. Lamme, V. A. F., Zipser, K. & Spekreijse, H. Figure-ground activity in primary visual cortex is suppressed by anesthesia. *Proc. Natl Acad. Sci.* **95**, 3263–3268 (1998).
42. Raz, A. et al. Preferential effect of isoflurane on top-down vs. bottom-up pathways in sensory cortex. *Front. Syst. Neurosci.* **8**, 191 (2014).

43. Chowdhury, S. A. & DeAngelis, G. C. Fine discrimination training alters the causal contribution of Macaque area MT to depth perception. *Neuron* **60**, 367–377 (2008).

44. Chen, N., Cai, P., Zhou, T., Thompson, B. & Fang, F. Perceptual learning modifies the functional specializations of visual cortical areas. *Proc. Natl Acad. Sci. USA* **113**, 5724–5729 (2016).

45. Chang, D. H. F., Mevorach, C., Kourtzi, Z. & Welchman, A. E. Training transfers the limits on perception from parietal to ventral cortex. *Curr. Biol.* **24**, 2445–2450 (2014).

46. Sale, A. et al. Visual perceptual learning induces long-term potentiation in the visual cortex. *Neuroscience* **172**, 219–225 (2011).

47. Wang, Q. & Burkhalter, A. Area map of mouse visual cortex. *J. Comp. Neurol.* **502**, 339–357 (2007).

48. Wang, Q., Sporns, O. & Burkhalter, A. Network analysis of cortico-cortical connections reveals ventral and dorsal processing streams in mouse visual cortex. *J. Neurosci.* **32**, 4386–4399 (2012).

49. Oh, S. W. et al. A mesoscale connectome of the mouse brain. *Nature* **508**, 207–214 (2014).

50. Morimoto, M. M., Uchishiba, E. & Saleem, A. B. Organization of feedback projections to mouse primary visual cortex. *iScience* **24**, 102450 (2021).

51. Wang, Q., Gao, E. & Burkhalter, A. Gateways of ventral and dorsal streams in mouse visual cortex. *J. Neurosci.* **31**, 1905–1918 (2011).

52. Winters, B. D., Forwood, S. E., Cowell, R. A., Saksida, L. M. & Bussey, T. J. Double dissociation between the effects of peri-postrhinal cortex and hippocampal lesions on tests of object recognition and spatial memory: heterogeneity of function within the temporal lobe. *J. Neurosci.* **24**, 5901–5908 (2004).

53. Winters, B. D. & Reid, J. M. A distributed cortical representation underlies crossmodal object recognition in rats. *J. Neurosci.* **30**, 6253–6261 (2010).

54. Jin, M. & Glickfeld, L. L. Mouse higher visual areas provide both distributed and specialized contributions to visually guided behaviors. *Curr. Biol.* **30**, 4682–4692.e7 (2020).

55. Goldbach, H. C., Akitake, B., Leedy, C. E. & Histed, M. H. Performance in even a simple perceptual task depends on mouse secondary visual areas. *eLife* **10**, e62156 (2021).

56. Porciatti, V., Pizzorusso, T. & Maffei, L. The visual physiology of the wild type mouse determined with pattern VEPs. *Vis. Res.* **39**, 3071–3081 (1999).

57. Cancedda, L. et al. Acceleration of visual system development by environmental enrichment. *J. Neurosci.* **24**, 4840–4848 (2004).

58. Fagiolini, M., Pizzorusso, T., Berardi, N., Domenici, L. & Maffei, L. Functional postnatal development of the rat primary visual cortex and the role of visual experience: dark rearing and monocular deprivation. *Vis. Res.* **34**, 709–720 (1994).

59. Pizzorusso, T., Fagiolini, M., Porciatti, V. & Maffei, L. Temporal aspects of contrast visual evoked potentials in the pigmented rat: effect of dark rearing. *Vis. Res.* **37**, 389–395 (1997).

60. Hubel, D. H. & Wiesel, T. N. Receptive fields, binocular interaction and functional architecture in the cat's visual cortex. *J. Physiol.* **160**, 106–154 (1962).

61. Prusky, G. T., West, P. W. & Douglas, R. M. Behavioral assessment of visual acuity in mice and rats. *Vis. Res.* **40**, 2201–2209 (2000).

62. Baroncelli, L. et al. Enriched experience and recovery from amblyopia in adult rats: impact of motor, social and sensory components. *Neuropharmacology* **62**, 2388–2397 (2012).

63. Bonaccorsi, J., Berardi, N. & Sale, A. Treatment of amblyopia in the adult: insights from a new rodent model of visual perceptual learning. *Front. Neural Circuits* **8**, 82 (2014).

64. Consorti, A. et al. Visual perceptual learning induces long-lasting recovery of visual acuity, visual depth perception abilities and binocular matching in adult amblyopic rats. *Front. Cell Neurosci.* **16**, 840708 (2022).

65. Fahle, M., Edelman, S. & Poggio, T. Fast perceptual learning in hyperacuity. *Vis. Res.* **35**, 3003–3013 (1995).

66. van Kerkoerle, T., Marik, S. A., Meyer zum Alten Borgloh, S. & Gilbert, C. D. Axonal plasticity associated with perceptual learning in adult macaque primary visual cortex. *Proc. Natl Acad. Sci.* **115**, 10464–10469 (2018).

67. Yang, T. & Maunsell, J. H. R. The effect of perceptual learning on neuronal responses in monkey visual area V4. *J. Neurosci.* **24**, 1617–1626 (2004).

68. Sanayei, M. et al. Perceptual learning of fine contrast discrimination changes neuronal tuning and population coding in macaque V4. *Nat. Commun.* **9**, 4238 (2018).

69. Tees, R. C. The effects of posterior parietal and posterior temporal cortical lesions on multimodal spatial and nonspatial competencies in rats. *Behav. Brain Res.* **106**, 55–73 (1999).

70. Weiss, Y., Edelman, S. & Fahle, M. Models of perceptual learning in vernier hyperacuity. *Neural Comput.* **5**, 695–718 (1993).

71. Dosher, B. & Lu, Z.-L. Visual perceptual learning and models. *Annu. Rev. Vis. Sci.* **3**, 343–363 (2017).

72. Ahissar, M. & Hochstein, S. Attentional control of early perceptual learning. *Proc. Natl Acad. Sci. USA* **90**, 5718–5722 (1993).

73. Ahissar, M. & Hochstein, S. The reverse hierarchy theory of visual perceptual learning. *Trends Cogn. Sci.* **8**, 457–464 (2004).

74. Hochstein, S. & Ahissar, M. View from the top: hierarchies and reverse hierarchies in the visual system. *Neuron* **36**, 791–804 (2002).

75. Ahissar, M., Nahum, M., Nelken, I. & Hochstein, S. Reverse hierarchies and sensory learning. *Philos. Trans. R. Soc. Lond. B: Biol. Sci.* **364**, 285–299 (2009).

76. Sasaki, Y., Nanez, J. E. & Watanabe, T. Advances in visual perceptual learning and plasticity. *Nat. Rev. Neurosci.* **11**, 53–60 (2010).

77. Lu, Z.-L. & Dosher, B. A. Current directions in visual perceptual learning. *Nat. Rev. Psychol.* **1**, 654–668 (2022).

78. Li, W. Perceptual learning: use-dependent cortical plasticity. *Annu. Rev. Vis. Sci.* **2**, 109–130 (2016).

79. Feinberg, E. H. & Meister, M. Orientation columns in the mouse superior colliculus. *Nature* **519**, 229–232 (2015).

80. Furtak, S. C., Ahmed, O. J. & Burwell, R. D. Single neuron activity and theta modulation in postrhinal cortex during visual object discrimination. *Neuron* **76**, 976–988 (2012).

81. Burgess, C. R. et al. Hunger-dependent enhancement of food cue responses in mouse postrhinal cortex and lateral amygdala. *Neuron* **91**, 1154–1169 (2016).

82. Gonchar, Y. & Burkhalter, A. Differential subcellular localization of forward and feedback interareal inputs to parvalbumin expressing GABAergic neurons in rat visual cortex. *J. Comp. Neurol.* **406**, 346–360 (1999).

83. Gonchar, Y. & Burkhalter, A. Distinct GABAergic targets of feedforward and feedback connections between lower and higher areas of rat visual cortex. *J. Neurosci.* **23**, 10904–10912 (2003).

84. Gilbert, C. D., Sigman, M. & Crist, R. E. The neural basis of perceptual learning. *Neuron* **31**, 681–697 (2001).

85. Vangeneugden, J. et al. Activity in lateral visual areas contributes to surround suppression in awake mouse V1. *Curr. Biol.* **29**, 4268–4275.e7 (2019).

86. Nurminen, L., Merlin, S., Bijanzadeh, M., Federer, F. & Angelucci, A. Top-down feedback controls spatial summation and response amplitude in primate visual cortex. *Nat. Commun.* **9**, 2281 (2018).

87. Bastos, A. M. et al. Canonical microcircuits for predictive coding. *Neuron* **76**, 695–711 (2012).

88. Mazziotti, R. et al. Mir-132/212 is required for maturation of binocular matching of orientation preference and depth perception. *Nat. Commun.* **8**, 15488 (2017).

Author contributions

A.C. contributed to conceive the experiments, performed the experiments, analyzed the data and contributed to the preparation of the manuscript. G.S. contributed to conceive the experiments, performed the experiments, and analyzed the data. I.D.M. and E.N. contributed to the immunohistochemical analyses. S.F. contributed to the behavioral experiments. N.B. contributed to conceive the experiments and to write the manuscript. A.S. conceived the experiments and wrote the manuscript. All authors have read and agreed to the published version of the manuscript.

Competing interests

The authors declare no competing interests.

Additional information

Supplementary information The online version contains supplementary material available at https://doi.org/10.1038/s41467-024-51817-5.

Correspondence and requests for materials should be addressed to Alessandro Sale.

Peer review information *Nature Communications* thanks Rinaldo D'Souza, Anthony Hannan and Dario Ringach for their contribution to the peer review of this work. A peer review file is available.

Reprints and permissions information is available at http://www.nature.com/reprints

Publisher's note Springer Nature remains neutral with regard to jurisdictional claims in published maps and institutional affiliations.